Inhibition of EZH2 transactivation function sensitizes solid tumors to genotoxic stress

Yiji Liao[a,1], Chen-Hao Chen[b,c,d,1], Tengfei Xiao[b,e], Bárbara de la Peña Avalos[f], Eloise V. Dray[f], Changmeng Cai[g], Shuai Gao[g], Neel Shah[b,e], Zhao Zhang[a], Avery Feit[b,h], Pengya Xue[a], Zhijie Liu[a], Mei Yang[a], Ji Hoon Lee[a], Han Xu[b,c], Wei Li[b,c], Shenglin Mei[b], Roodolph S. Pierre[h,i], Shaokun Shu[b,e], Teng Fei[b,e], Melissa Duarte[b], Jin Zhao[b,e], James E. Bradner[h,i], Kornelia Polyak[b,e], Philip W. Kantoff[b,e], Henry Long[b], Steven P. Balk[j], X. Shirley Liu[b,c,d,2], Myles Brown[b,e,2], and Kexin Xu[a,b,2]

[a]Department of Molecular Medicine, University of Texas Health Science Center at San Antonio, San Antonio, TX 78229; [b]Center for Functional Cancer Epigenetics, Dana-Farber Cancer Institute, Boston, MA 02115; [c]Department of Data Science, Dana-Farber Cancer Institute, Boston, MA 02115; [d]Department of Biostatistics, Harvard T.H. Chan School of Public Health, Boston, MA 02115; [e]Department of Medical Oncology, Dana-Farber Cancer Institute, Harvard Medical School, Boston, MA 02115; [f]Department of Biochemistry and Structural Biology, University of Texas Health Science Center at San Antonio, San Antonio, TX 78229; [g]Center for Personalized Cancer Therapy, University of Massachusetts, Boston, MA 02125; [h]Department of Medicine, Brigham and Women's Hospital, Harvard Medical School, Boston, MA 02115; [i]Biological and Biomedical Science Program, Harvard Medical School, Boston, MA 02115; and [j]Hematology-Oncology Division, Department of Medicine, Beth Israel Deaconess Medical Center, Boston, MA 02115

Contributed by Myles Brown; received April 9, 2021; accepted December 2, 2021; reviewed by Alfred Sze-Lok Cheng, Chia-Lin Wei, and Jindan Yu

Drugs that block the activity of the methyltransferase EZH2 are in clinical development for the treatment of non-Hodgkin lymphomas harboring EZH2 gain-of-function mutations that enhance its polycomb repressive function. We have previously reported that EZH2 can act as a transcriptional activator in castration-resistant prostate cancer (CRPC). Now we show that EZH2 inhibitors can also block the transactivation activity of EZH2 and inhibit the growth of CRPC cells. Gene expression and epigenomics profiling of cells treated with EZH2 inhibitors demonstrated that in addition to derepressing gene expression, these compounds also robustly down-regulate a set of DNA damage repair (DDR) genes, especially those involved in the base excision repair (BER) pathway. Methylation of the pioneer factor FOXA1 by EZH2 contributes to the activation of these genes, and interaction with the transcriptional coactivator P300 via the transactivation domain on EZH2 directly turns on the transcription. In addition, CRISPR-Cas9–mediated knockout screens in the presence of EZH2 inhibitors identified these BER genes as the determinants that underlie the growth-inhibitory effect of EZH2 inhibitors. Interrogation of public data from diverse types of solid tumors expressing wild-type EZH2 demonstrated that expression of DDR genes is significantly correlated with EZH2 dependency and cellular sensitivity to EZH2 inhibitors. Consistent with these findings, treatment of CRPC cells with EZH2 inhibitors dramatically enhances their sensitivity to genotoxic stress. These studies reveal a previously unappreciated mechanism of action of EZH2 inhibitors and provide a mechanistic basis for potential combination cancer therapies.

EZH2 inhibitors | DNA damage repair | mechanism of drug action | cancer therapy

The methyltransferase EZH2 has shown encouraging therapeutic potential in cancer (1). Originally identified as the catalytic subunit of the polycomb repressive complex 2 (PRC2), EZH2 methylates histone H3 at lysine 27 (H3K27) and leads to gene silencing (2). EZH2 is frequently up-regulated in a broad spectrum of aggressive solid tumors and its overabundance is significantly associated with poor prognosis (3). Gain-of-function mutations at residues Y641, A677, or A687 within the catalytic domain of EZH2 have been identified in diffuse large B-cell lymphoma (DLBCL) and follicular lymphoma (FL) (4, 5). In view of these oncogenic features of EZH2, several selective inhibitors that block EZH2 enzymatic activity were developed (6–8). These compounds specifically inhibit EZH2-mediated methyltransferase activities by competing with the methyl donor *S*-adenosylmethionine for the binding pocket inside the catalytic domain. These prototype drugs abrogate the growth of non-Hodgkin lymphoma (NHL) cells that harbor EZH2 driver mutations, decrease global trimethylation of H3K27 (H3K27me3), and reactivate genes that are repressed by the PRC2 complex. However, it remains unclear whether the efficacy of EZH2 inhibitors will be limited to NHL harboring gain-of-function mutations or will be efficacious as well on other solid tumors without somatic mutations of EZH2.

Genotoxic stress, such as that induced by radiation or chemotherapy, predisposes cells to DNA damages and elicits

Significance

We identified a group of DNA repair genes directly induced by EZH2 and repressed by EZH2 inhibitors. Expression of these genes predicts the response of wild-type EZH2-harboring solid tumors to EZH2 inhibitors. Most importantly, our findings lay the foundation for the development of a combination therapy that combines EZH2 inhibitors and DNA damaging agents or drugs that block DNA repair for the treatment of castration-resistant prostate cancer and other solid tumors.

Author contributions: C.-H.C., E.V.D., N.S., K.P., P.W.K., S.P.B., X.S.L., M.B., and K.X. designed research; Y.L., C.-H.C., T.X., B.d.l.P.A., S.G., N.S., M.Y., J.H.L., R.S.P., S.S., T.F., M.D., J.Z., and K.X. performed research; P.X., Z.L., and J.E.B. contributed new reagents/analytic tools; Y.L., C.-H.C., T.X., B.d.l.P.A., E.V.D., N.S., Z.Z., A.F., H.X., W.L., S.M., H.L., S.P.B., X.S.L., M.B., and K.X. analyzed data; Y.L., C.-H.C., X.S.L., M.B., and K.X. wrote the paper; R.S.P., S.S., and T.F. provided technical instructions and assistance; and J.E.B., K.P., P.W.K., H.L., and S.P.B. provided technical instructions and intellectual advice.

Reviewers: A.S.-L.C., The Chinese University of Hong Kong; C.-L.W., The Jackson Laboratory; and J.Y., Northwestern University.

Competing interest statement: N.S. receives research grant funding from AstraZeneca. J.E.B. is an executive and shareholder of Novartis AG and has been a founder and shareholder of SHAPE (acquired by Medivir), Acetylon (acquired by Celgene), Tensha (acquired by Roche), Syros, Regency, and C4 Therapeutics. P.W.K. serves on the scientific advisory board (SAB) of BIND Biosciences, BN Immunotherapeutics, GE Healthcare, Janssen, New England Research Institutes, OncoCellMDX, Progenity, Sanofi, and Thermo Fisher. He shares investment interests in Context Therapeutics, Druggability Technologies Holdings Ltd. (DRGT), Placon, Seer Biosciences, and Tarveda Therapeutics. He also serves on the Data and Safety Monitoring Board (DSMB) of Genetech and Merck. X.S.L. is a cofounder, board member, SAB, and consultant of GV20 Oncotherapy and its subsidiaries. M.B. is a consultant to and receives sponsored research support from Novartis and is a consultant to MPM Capital and serves on the SAB of Kronos Bio, H3 Biomedicine, and GV20 Oncotherapy.

[1]Y.L. and C.-H.C. contributed equally to this work.

[2]To whom correspondence may be addressed. Email: xsliu@ds.dfci.harvard.edu, myles_brown@dfci.harvard.edu, or xuk3@uthscsa.edu.

This article contains supporting information online at http://www.pnas.org/lookup/suppl/doi:10.1073/pnas.2105898119/-/DCSupplemental.

Published January 14, 2022.

diverse biological responses, including DNA repair, cell-cycle arrest, and apoptosis (9). Deregulation of components critical for an appropriate DNA damage response leads to genome instability, a hallmark of most cancers. Therefore, drugs that induce DNA damage or inhibit DNA damage response, such as cisplatin and PARP inhibitors, are effective anticancer agents across a wide array of tumor types. Growing evidence suggests that EZH2 plays a pivotal role in determining how cancer cells respond to DNA damage. For instance, knockdown of EZH2 predominantly induced apoptosis in both p53-proficient and -deficient cancer cells. This was dependent on H3K27me3-mediated epigenetic silencing of *FBXO32*, which is required for p21 protein degradation (10). Another report shows that depletion of EZH2 rapidly prompted senescence via activation of ATM-p53-p21 pathway. Interestingly, no changes in the pattern or overall levels of H3K27me3 were observed during the process (11). These studies present a diverse and complex picture of EZH2 functions in regulation of DNA damage response. Additionally, the role of H3K27me3 in these processes is unclear, raising the question of how exactly EZH2 triggers the specific biological responses to DNA damage. Conversely, it is largely unknown whether components involved in the DNA damage response, in return, influence the oncogenic functions of EZH2. Unraveling answers to these questions will have a profound impact on the development of EZH2 inhibitors and combination cancer therapies.

In this study, we comprehensively evaluated and confirmed the therapeutic potentials of EZH2 inhibition in solid tumors that express wild-type EZH2, using prostate cancer cell models. Specifically, we found a mechanism of action of EZH2 inhibitors in cancers without EZH2 somatic mutations, which involves down-regulation of a specific set of DNA damage repair (DDR) genes that are directly activated by the FOXA1–EZH2–P300 axis. Our results suggest that DNA repair mechanism might underlie the growth inhibitory effect of EZH2 inhibitors in cancer cells that express wild-type EZH2. More importantly, EZH2 inhibitors potentiated the activity of DNA-damaging agents and synergistically blocked the growth of advanced prostate cancer cells. Therefore, our work elucidates a mechanism of action of EZH2 inhibitors in solid tumors and suggests potential combination therapies.

Results

EZH2 Inhibitors Suppress the Proliferation of Androgen Receptor–Positive Prostate Cancer Cells. To determine the gene(s) essential for the sustained proliferation of androgen-dependent and castration-resistant prostate cancer (CRPC) cells, we conducted a CRISPR-Cas9 knockout screen in both parental hormone-dependent LNCaP cells and its hormone-refractory counterpart LNCaP-abl (abl) cells under their respective proliferating conditions (Fig. 1*A*). Positive control genes that are known to be required for cell proliferation in general were strongly selected, suggesting that the screens could reliably identify essential genes (*SI Appendix*, Fig. S1*A*). We used MAGeCK (12, 13) to analyze the CRISPR screen data, which assigns a beta (β) score to each gene to approximate the log fold change of CRISPR guide DNA abundance. Therefore, in the cells grown for 4 wk compared with those on day 0, a more negative β score represents higher dependency of cell growth on the target gene. We were particularly interested in genes that are more essential for the androgen-independent growth of CRPC cells, so we compared the β scores between LNCaP and abl. Although most genes possessed similar β scores between these two prostate cancer cell lines, we did find some, which are well known for their prominent roles in CRPC (14), showing significantly lower scores in abl than in LNCaP (Fig. 1*B*). Interestingly, EZH2 was one of the top hits that exhibit much stronger dependency in abl cells than in LNCaP (*SI Appendix*, Fig. S1*B*), while EZH1, another mammalian homolog of *Drosophila* Enhancer of Zeste, was not required for either cell line. This result is consistent with our previous report that genetic inhibition of EZH2 better suppresses growth of CRPC cells than that of androgen-dependent prostate cancer cells (15).

We then assessed the efficacy of EZH2 inhibitors (EZH2i) in prostate cancer cells. We tested two compounds, GSK126 (GSK) (6) and EPZ-6438 (EPZ) (7), in a panel of human prostate cell lines, including two benign prostate epithelial cells, two androgen receptor (AR)-null prostate cancer cells, and eight AR-positive cancer cells. Only malignant cells with intact AR signaling, especially the hormone-refractory lines, were sensitive to both inhibitors (Fig. 1*C*). Concentrations as low as 500 nM of EZH2i greatly retarded the growth of castration-resistant abl cells (Fig. 1*D*), and relatively higher doses of EZH2i were required to suppress the androgen-dependent LNCaP cells (Fig. 1*E*). The inhibitory effect of EZH2i was minimal in AR-null DU145 (*SI Appendix*, Fig. S1*C*). Cell-cycle analysis showed that EZH2i induced G0–G1 arrest in responsive CRPC cell lines within 3 d of the drug treatment (*SI Appendix*, Fig. S1*D*), but not in the unresponsive DU145 cells (*SI Appendix*, Fig. S1*E*). To further evaluate EZH2i's effect on CRPC cell growth in vivo, we treated subcutaneous xenografts of the hormone-refractory CWR22Rv1 cells in castrated mice with either GSK126 (Fig. 1*F*) or EPZ-6438 (Fig. 1*G*). Both compounds significantly retarded tumor growth following three weeks of treatment. Taken together, we demonstrated that EZH2 is a promising therapeutic target for prostate cancer and that EZH2 inhibitors may benefit patients with AR-positive, metastatic, hormone-refractory tumors.

EZH2 Inhibition Induces a Specific Gene Signature in Sensitive CRPC Cells. To investigate the mechanisms underlying the action of EZH2i in sensitive prostate cancer cells, we profiled the gene expression pattern in abl cells upon the treatment with GSK126 or EPZ-6438 (*SI Appendix*, Fig. S2*A*). Interestingly, in addition to transcriptional derepression, we found a large number of genes significantly down-regulated upon EZH2i treatment. Genes that were commonly down-regulated by both EZH2i in abl cells were significantly enriched in various DNA repair pathways (Fig. 2*A*). In contrast, there were no significant functional annotations for the up-regulated genes in abl. To rule out the possible off-target effect of EZH2i on gene regulation, we carried out two analyses. First, we compared the transcriptional profiles in abl treated with EZH2i or transfected with EZH2-targeting RNA interference (15) and observed highly similar gene expression patterns (Fig. 2*B*). Second, we carried out gene expression profiling in EZH2i-insensitive DU145 cells after genetic and pharmacological inhibition of EZH2 (*SI Appendix*, Fig. S2*B*). Again, genes that were differentially expressed after EZH2i treatment were also changed by EZH2 knockdown in the same direction, especially those that are up-regulated upon EZH2 inhibition. However, the commonly down-regulated genes in DU145 were not enriched in any functional annotations that were seen for those down-regulated by EZH2 inhibition in abl (*SI Appendix*, Fig. S2*C*). We validated several EZH2i-down-regulated genes in abl cells and showed that EZH2i suppressed their expression in a dose- (*SI Appendix*, Fig. S2*D*) and time-dependent manner (*SI Appendix*, Fig. S2*E*). We further examined the expression of these genes in three other EZH2i-sensitive CRPC cell lines (Fig. 2*C*). Not only did GSK126 and EPZ-6438 up-regulate EZH2-repressed genes, they also down-regulated the expression of EZH2-activated genes in these cells. We further validated these findings in CWR22Rv1 xenografts, demonstrating consistent decrease in messenger RNA (mRNA) (Fig. 2*D*) and protein (Fig. 2*E*) levels of EZH2-activated genes by either compound. Taken

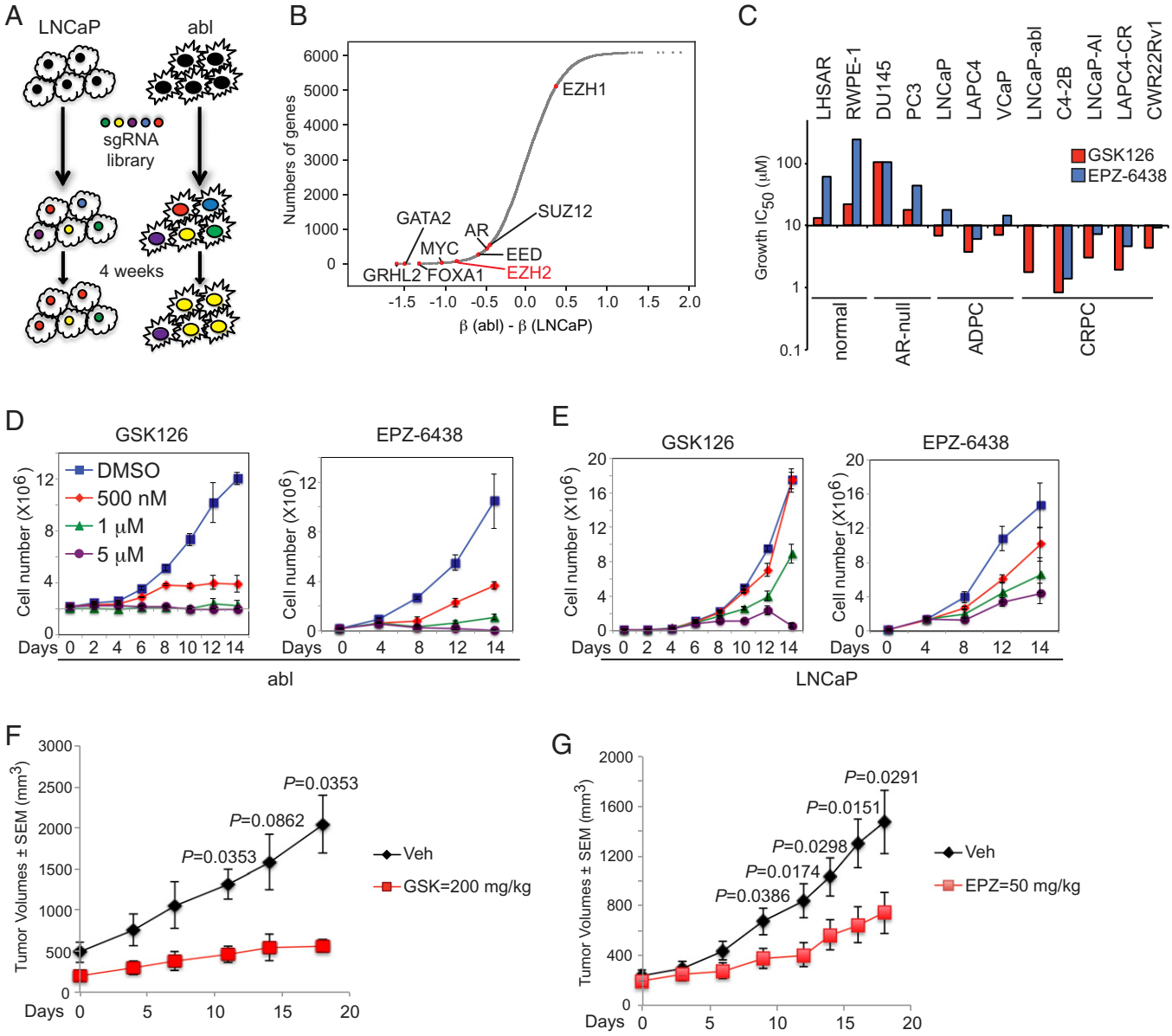

Fig. 1. EZH2 inhibitors showed potent inhibitory effects in prostate cancer cells, especially the castration-resistant ones. (*A*) Workflow of CRISPR knockout screens in LNCaP and abl cells. (*B*) Differential gene essentiality represented by difference of beta (β) scores between abl and LNCaP [β (abl) − β (LNCaP)]. Positions of representative genes were indicated by red dots. (*C*) IC_{50} values of two EZH2 inhibitors in prostate normal and cancer cell lines after 6 d of treatment. ADPC, androgen-dependent prostate cancer. (*D* and *E*) Effects of EZH2 inhibitors on cell growth in abl (*D*) and LNCaP (*E*). (*F* and *G*) Growth curves of xenograft tumors in castrated nude mice injected with CWR22Rv1 cells receiving vehicle (Veh) or EZH2 inhibitors (*F*, GSK126; *G*, EPZ-6438).

together, we identified a group of DDR genes that are downregulated upon inhibition of EZH2.

EZH2i-Resistance Mutations Rescue the Effects of EZH2 Inhibitors on Gene Expression and Cell Growth in Prostate Cancer Cells. Secondary mutations in EZH2, like Y111D and Y661D, were identified in DLBCL clones that became refractory to EZH2i (16, 17). These resistance mutants offer a genetic means to evaluate the targeted action of EZH2i. Thus, we replaced the endogenous EZH2 in CRPC abl cells with these mutants and then evaluated the effects of EZH2i on H3K27me3 levels. When either Y111D or Y661D was expressed, EZH2i-induced reduction of H3K27me3 level was dramatically alleviated (Fig. 3*A*). In cell growth assays, both GSK126 (*SI Appendix*, Fig. S3*A*) and EPZ-6438 (*SI Appendix*, Fig. S3*B*) failed to suppress the growth of abl cells expressing Y111D or Y661D, displaying a much higher IC_{50} (concentration that exhibits 50% of the maximal inhibitory effect) value than in the control cells or cells expressing wild-type EZH2 (Fig. 3*B*). There was no inhibitory effect even after incubation with the drugs for up to 15 d (Fig. 3*C*). These results demonstrated that EZH2 mutations that render EZH2i resistance in DLBCL also confer similar refractory phenotype in prostate cancer cells. Intriguingly, EZH2i-induced derepression of EZH2-repressed genes was diminished only in the presence of Y111D but not Y661D (*SI Appendix*, Fig. S3*C*). In contrast, the effect of EZH2i on EZH2-activated DDR genes was remarkably mitigated by both mutants, which is more consistent with the observation that both Y111D and Y661D rendered ineffectiveness of EZH2i in abl cells (Fig. 3*D*). These findings further support the inhibitory effect of EZH2i on cell growth through specific blockade of EZH2 functions, particularly its gene activation activity, in CRPC.

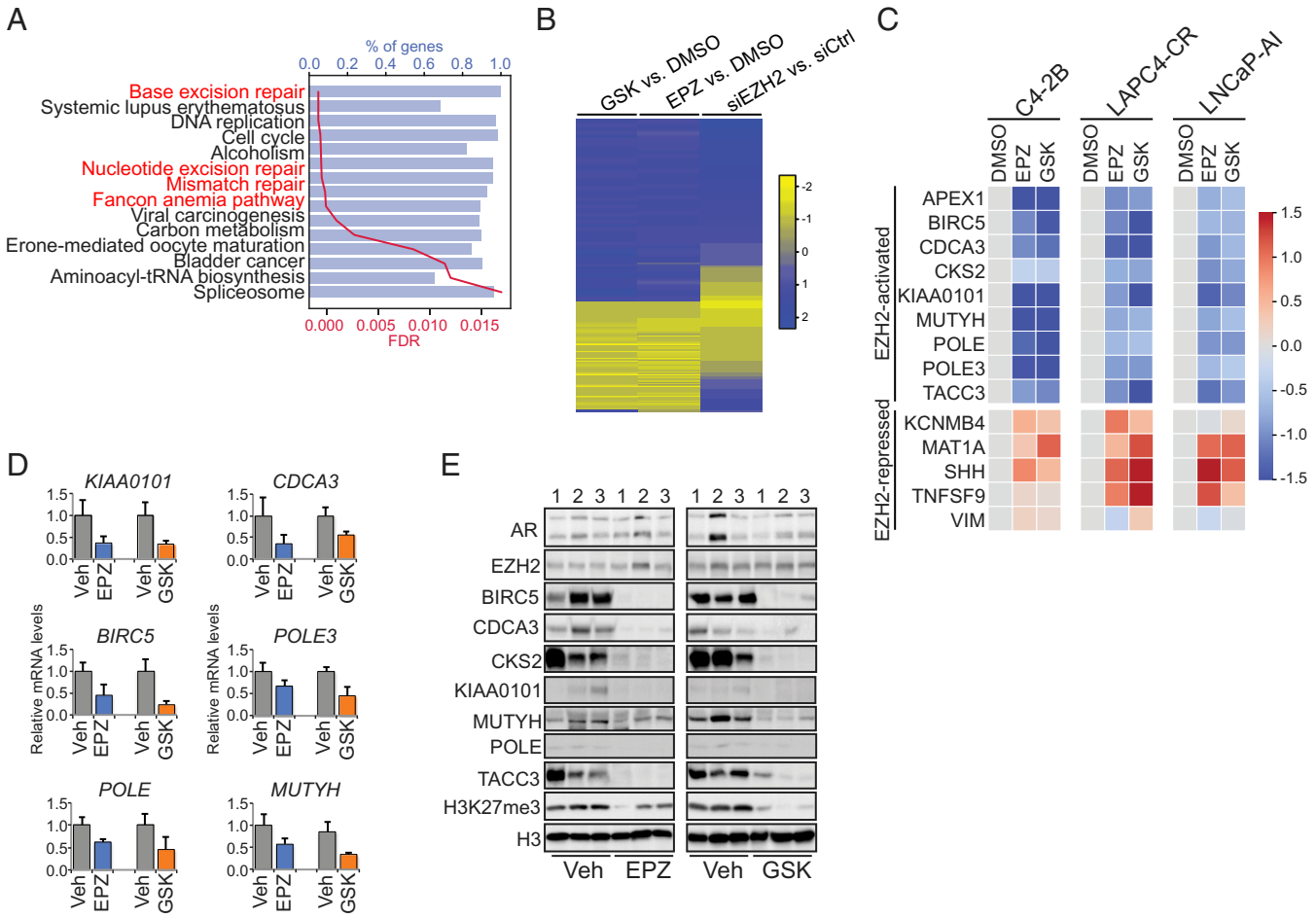

Fig. 2. EZH2 inhibitors down-regulated a large number of genes in sensitive CRPC cells. (*A*) KEGG pathways overrepresented in genes that were significantly down-regulated by EZH2 inhibitors in abl cells. FDR, false discovery rate. (*B*) Heat map of differential gene expression (Log2-transformed fold changes) induced by EZH2 inhibitors (GSK [EPZ] vs. DMSO) or EZH2 knockdown (siEZH2 vs. siCtrl) in abl cells. Gene expression profiling upon silencing EZH2 was retrieved from our prior work (15). (*C*) Heat maps of RT-qPCR results showing expression changes of selected genes in C4-2B, LAPC4-CR, and LNCaP-AI treated with DMSO or 5 μM EZH2 inhibitors for 72 h. (*D* and *E*) mRNA (*D*) and protein (*E*) levels of selected genes in xenograft tumor tissues from mice receiving vehicle (Veh) or EZH2 inhibitors. Numbers in *E* are triplicates of tissue samples.

EZH2 Inhibitors Decrease Global H3K27me3 Signals on Chromatin Regardless of Cellular Response to the Compounds. In view of the canonical function of EZH2 in catalyzing H3K27me3, we set out to investigate how the repressive histone mark contributes to the gene-regulatory effects of EZH2i. Despite differential sensitivity to EZH2i, all of the tested prostate cell lines demonstrated reduced total H3K27 di- and trimethylation levels upon EZH2i treatment in a dose-dependent manner (Fig. 4*A*). To accurately evaluate the locus-specific changes of H3K27me3 on chromatin, we adopted the ChIP-Rx method, which uses a "SPIKE-IN" strategy to quantify genome-wide histone modification relative to a reference epigenome with defined quantities (18). In short, we added equal amounts of *Drosophila* chromatin into different groups of chromatin immunoprecipitation (ChIP) samples and then constructed H3K27m3 ChIP-sequencing (ChIP-seq) libraries using the mixture of chromatin. Canonical normalization methods such as using the total sequencing reads showed moderate H3K27me3 changes after cells were treated with EZH2i (*SI Appendix*, Fig. S4 *A* and *B*), while normalization to the SPIKE-IN epigenome by correcting the sequencing reads from human samples based on the ratios of read counts from *Drosophila* chromatin in treatment group to those in control group showed remarkable H3K27me3 reductions (Fig. 4*B*). In EZH2i-insensitive DU145 cells, we noticed a similar decrease of global H3K27me3 signals on chromatin induced by EZH2i as in the EZH2i-sensitive abl cells (Fig. 4*C*). Actually, the H3K27me3 signals at gene-specific chromatin loci were more sensitive to EZH2i treatment in DU145 than in abl, as H3K27me3 levels at promoters of selected genes were decreased after 5 d of EZH2i treatment in abl (Fig. 4*D*) but as early as 2 d in DU145 (*SI Appendix*, Fig. S4*C*). All these results imply that H3K27me3 reduction alone does not confer cellular sensitivity to EZH2i.

To find any functional significance of EZH2i-triggered H3K27me3 alterations in abl cells, we associated changes of the repressive histone mark with differential gene expression upon compound treatment (Fig. 4*E*). Although the basal level of H3K27me3 was noticeably higher at the promoter regions of EZH2i-up-regulated genes, there were no differences regarding the extent of H3K27me3 decrease among EZH2-repressed, -activated, or -unregulated genes. This result suggests that while steady H3K27me3 level is associated with transcription silencing, signal changes of this histone mark do not always associate with immediate transcriptional changes of nearby genes. Taken together, our results suggest that H3K27 methylation, a readout of the polycomb repressive function of EZH2, may not be the determining factor of transcriptional changes or cellular responses to EZH2i.

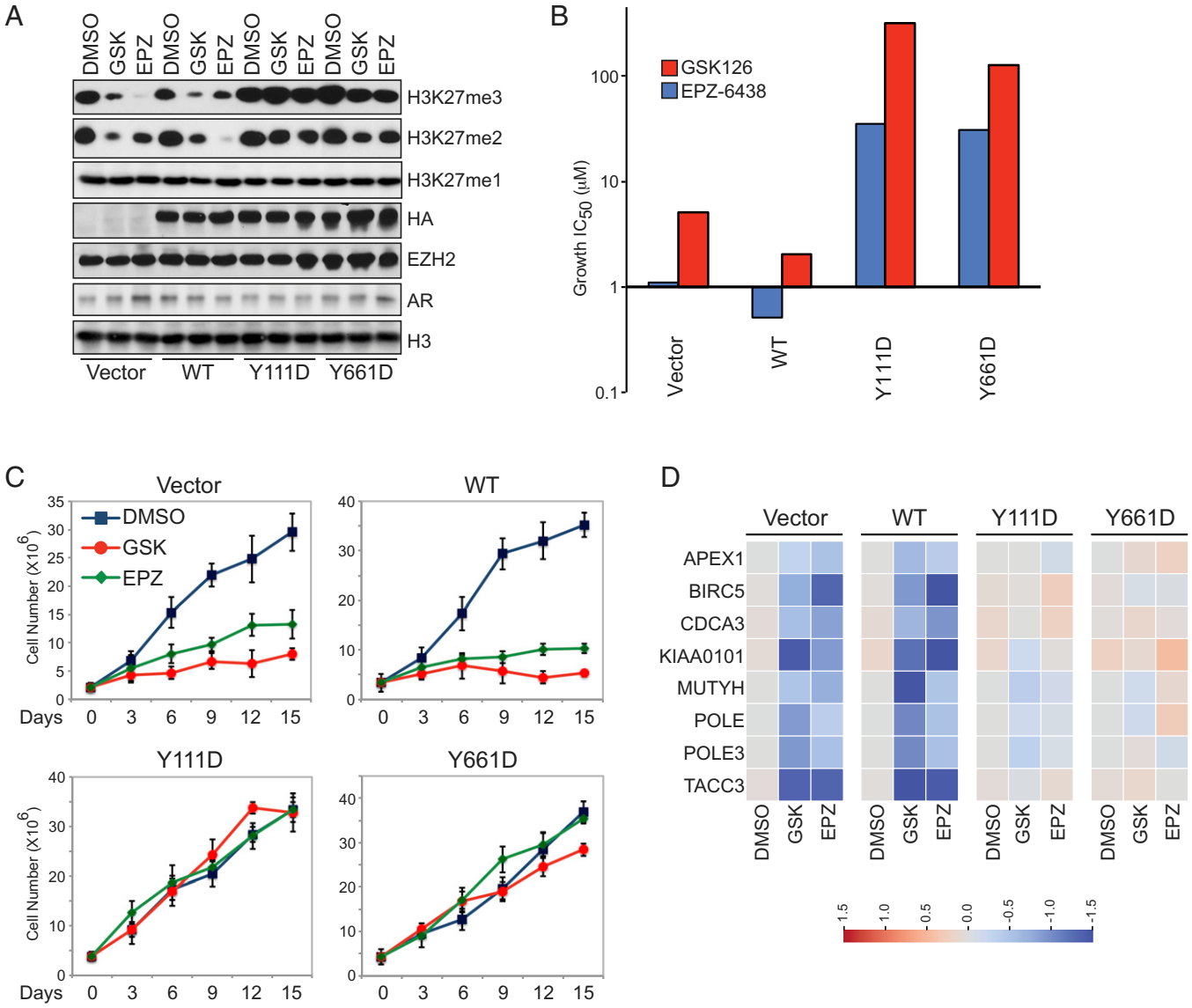

Fig. 3. Genetic mutations of EZH2 conferred resistance to EZH2 inhibitors. (*A*) Western blot in abl cells where the endogenous EZH2 was replaced with the empty vector control (Vector), the wild-type (WT), or mutant (Y111D or Y661D) EZH2 after incubation with 5 μM EZH2 inhibitors for 72 h. (*B*) IC_{50} values of two EZH2 inhibitors in abl cells as described in *A* upon treatment for 6 d. (*C*) Growth of abl cells as described in *A* in the presence of 1 μM EZH2 inhibitors. (*D*) Heat map showing expression changes of indicated genes in abl cells as described in *A* after incubation with 5 μM EZH2 inhibitors for 3 d.

Methylation of FOXA1 and EZH2 TAD-P300 Interaction Both Contribute to EZH2-Mediated Direct Transactivation of the DDR Genes. To investigate how EZH2 transcriptionally activates DDR genes in CRPC cells regardless of the H3K27me3 status at their promoters, we first knocked down SUZ12 and EED and found that some of the tested DDR genes were down-regulated in abl cells (*SI Appendix*, Fig. S5*A*) but none of them were changed in DU145 (*SI Appendix*, Fig. S5*B*), even though EZH2-repressed genes were all up-regulated in the knockdown cells. These results indicate that EZH2-mediated transactivation of the DDR genes needs optimal methyltransferase activity of EZH2. Recently, FOXA1 was reported to be methylated by EZH2 at K295, which stabilizes the pioneer factor and activates cell-cycle genes (19). Therefore, we replaced the endogenous FOXA1 in abl cells with the wild-type protein or the K295R mutant that can no longer be methylated by EZH2 (Fig. 5*A*). Only overexpression of the intact FOXA1, but not the mutant one, restored FOXA1 knockdown-induced down-regulation of the selected DDR genes. Transcription of these genes was all silenced upon GSK126 treatment, regardless of FOXA1 mutation status (Fig. 5*B*). This indicates that EZH2-catalyzed methylation of the nonhistone substrate FOXA1 is involved in down-regulation of the DDR genes by EZH2i.

We previously reported that phosphorylation of EZH2 at S21 serves as a functional switch of EZH2 from a polycomb repressor to a transcriptional coactivator for AR in CRPC cells (15). In an independent study (20), a transactivation domain (TAD) was identified on EZH2 protein, which helps release EZH2 from the PRC2 complex and interact with P300. Therefore, we first silenced *EP300* in abl cells and found that expression of the DDR genes was dramatically decreased to the levels seen in the EZH2i-treated cells (*SI Appendix*, Fig. S5*C*). Second, we substituted the endogenous EZH2 in abl cells with the intact protein or a TAD-defective mutant that loses the ability

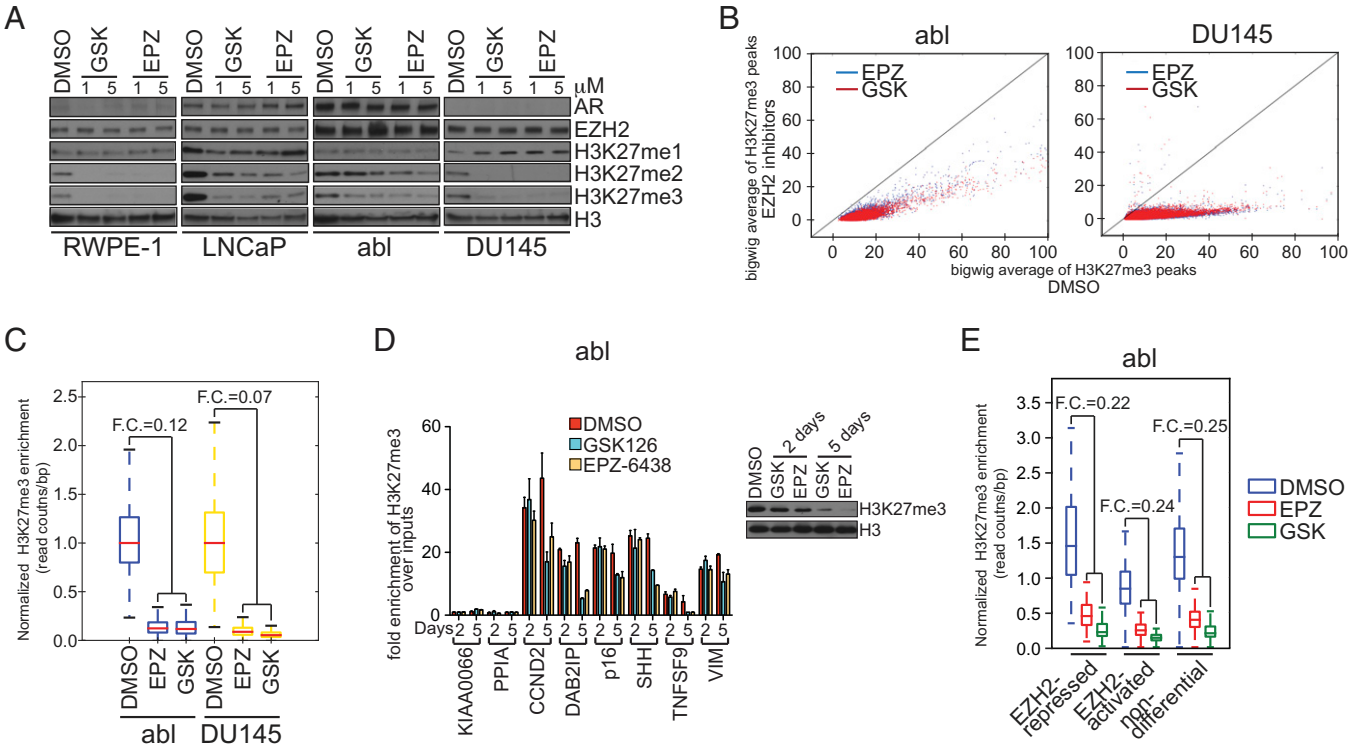

Fig. 4. Reduction in H3K27 trimethylation levels did not dictate the action of EZH2 inhibitors in prostate cancer cells. (*A*) Western blot in prostate cell lines after treatment with 1 or 5 μM EZH2 inhibitors for 3 d. (*B*) Scatter plots of H3K27me3 peak signals, normalized with the SPIKE-IN epigenome, in abl and DU145 cells after treatment with 5 μM EZH2 inhibitors for 3 d. Each dot represents one H3K27me3 peak called under the DMSO treatment condition. (*C*) Comparison of EZH2 inhibitor-induced changes of H3K27me3 levels between abl and DU145 cells after SPIKE-IN normalization. F.C., fold change. (*D*) ChIP-qPCR of H3K27me3 in abl cells treated with 5 μM EZH2 inhibitors. Promoters of *KIAA0066* and *PPIA*, negative controls (15); (*Right*) immunoblotting in ChIP samples. (*E*) SPIKE-IN normalized changes of H3K27me3 peak signals upon EZH2 inhibitor treatment at the gene body regions of EZH2-repressed (n = 75), -activated (n = 147), or -unregulated (nondifferential, n = 12,659) genes. F.C., fold change.

to recruit P300 (Fig. 5*C*). The levels of AR protein were reduced upon EZH2 knockdown, which is consistent with previous findings that EZH2 induces AR transcription (21). We found, however, that this does not require the previously reported TAD of EZH2, as the TAD mutant EZH2 is also able to rescue the effect of EZH2 knockdown on AR expression to levels equivalent to wild-type EZH2. This further confirms the positive regulation of AR activity by EZH2 in CRPC cells. Wild-type EZH2, but not the mutant form, rescued the inhibitory effect of EZH2 knockdown on DDR gene expression, which was all diminished upon EZH2i treatment (Fig. 5*D*).

Based on these data, we speculated that EZH2-catalyzed methylation of the pioneer factor FOXA1 enables the chromatin environment to facilitate gene activation and the EZH2 TAD–P300 interaction, which occurs upon EZH2 phosphorylation at S21 in CRPC cells, turns on the transactivation activity of EZH2 and works together with AR to activate the DDR genes. Indeed, EZH2i-induced down-regulation of DDR genes was the most prominent in abl, much milder in LNCaP, and not observed in DU145 (*SI Appendix*, Fig. S5*D*), since both FOXA1 methylation and EZH2 phosphorylation happen only in abl, but not in LNCaP where EZH2 is not phosphorylated or in DU145, a FOXA1- and AR-negative prostate cancer cell line (22). Furthermore, substitution of the phosphorylation dead mutant S21A or the methyltransferase inactive mutant (15) for the endogenous EZH2 in abl cells failed to reverse the inhibitory effect of EZH2 knockdown on DDR gene expression (*SI Appendix*, Fig. S5*E*). These results further support that the enzymatic activity of EZH2, which is responsible for methylating FOXA1, and EZH2 phosphorylation at S21, which dictates the functional switch, contribute to the activation of the DDR genes.

We further showed that EZH2 peaks with low H3K27me3 signals were significantly enriched, whereas those colocalized with H3K27me3 mark were almost devoid, around these DDR genes (Fig. 5*E*). This is in agreement with a previous report that the EZH2 TAD–P300 interaction liberates the methyltransferase from the PRC2 complex and attenuates its activity toward H3K27 (20). In addition, based on the publicly available ChIP-seq data (23), we found that AR peak intensities at the enhancers of these DDR genes were higher in CRPC cell lines than in the androgen-dependent cell line LNCaP (*SI Appendix*, Fig. S6 *A* and *B*). Signals of AR peaks were positively correlated with EZH2 and H3K27ac peaks but not with H3K27me3 peaks (Fig. 5*F*). They showed a linear correlation with chromatin-binding intensities of EZH2 around DDR genes, and H3K27ac signals tended to increase at stronger EZH2-AR colocalization sites (Fig. 5*G*). Such correlations were modest in LNCaP cells (*SI Appendix*, Fig. S6 *C* and *D*). Finally, we detected similar levels of total EZH2 and FOXA1 in LNCaP and abl cells at enhancers of selected DDR genes, but noticeably more phosphorylated EZH2 and P300 in abl (Fig. 5*H*). Consistently, H3K27ac, which is catalyzed by P300 (24), was enriched at these enhancer regions in abl cells. More importantly, treatment with EZH2i dramatically impaired the chromatin association of all these factors. Taking all these data together, we concluded that activation of the DDR genes we identified are directly elicited through chromatin association of an EZH2-centered transcriptional network, including FOXA1, P300 and AR, in CRPC cells.

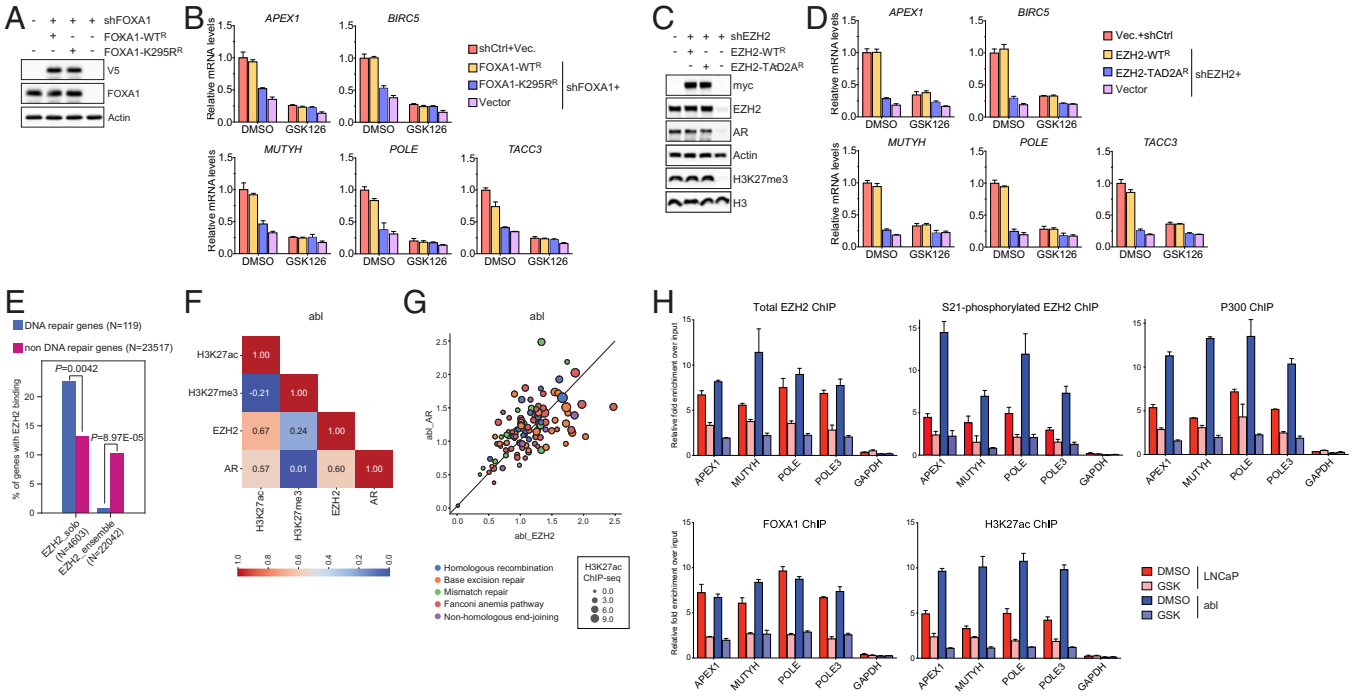

Fig. 5. Methylation of FOXA1 and TAD-P300 interaction both contribute to the direct transactivation of the DDR genes by EZH2. (*A–D*) Immunoblotting (*A* and *C*) and expression of selected genes (*B* and *D*) in abl cells where the endogenous FOXA1 (*A* and *B*) or EZH2 (*C* and *D*) was replaced with the wild-type protein or the indicated mutant form [FOXA1-K295R^R with a single point mutation K295R (19); EZH2-TAD2A^R with F171A/F224A double point mutations (20)]. DNA constructs expressing FOXA1 and EZH2 are V5- and myc-tagged, respectively, which contain synonymous substitutions rendering resistance to corresponding short hairpin RNAs (shRNAs). In *B* and *D*, cells were treated with 5 μM GSK126 for 72 h. (*E*) Percentages of genes containing EZH2_solo (EZH2 peaks with no or low H3K27me3 signals, $n = 4,603$) or EZH2_ensemble (EZH2 peaks with high H3K27me3 signals, $n = 22,042$) within ±1 kb of their transcriptional start sites. These two types of EZH2 peaks were retrieved and defined in our prior work (15). Blue bars, $n = 119$ (27 bound by EZH2_solo and 1 by EZH2_ensemble); rose red bars, $n = 23,517$ (3,110 bound by EZH2_solo and 2,397 by EZH2_ensemble). The *P* values were calculated using Fisher's exact test. (*F* and *G*) Spearman correlation among peak intensities (*F*) and ChIP-seq signals (*G*) of specified factors within 20 kb upstream from the transcriptional start sites of DDR genes in abl cells. (*H*) ChIP-qPCR of indicated factors in LNCaP and abl cells treated with 5 μM GSK126 for 72 h. Promoter region of *GAPDH* serves as a negative control.

A Core Gene Signature in Regulation of DNA Repair Is Essential for the Growth-Inhibitory Effects of EZH2 Inhibitors in Prostate Cancer. To identify the determinants underlying the inhibitory effects of EZH2i, we conducted CRISPR-Cas9 knockout screens in abl and LNCaP cells with or without GSK126 treatment (Fig. 6*A*). Again, MAGeCK assigned similar beta scores on most genes between treatment and control conditions in these two cell lines (*SI Appendix*, Fig. S7*A*). We postulated that knockout of genes crucial for the growth-inhibitory effect of EZH2i would render clones resistant to the compounds, so we defined a delta beta score (Δβ) as the difference in β scores between treatment (GSK126) and control (dimethyl sulfoxide, DMSO) groups. Genes with positive Δβ are required for EZH2i activity. This analysis identified a specific group of genes with positive Δβ score in abl cells, predominantly functioning in base excision repair (Fig. 6*B*). Similar analyses also identified some genes with positive Δβ values in LNCaP (*SI Appendix*, Fig. S7*B*). However, they were enriched in totally different functional annotations (*SI Appendix*, Fig. S7*C*). Indeed, there were comparable numbers of base excision repair (BER) genes with positive and negative Δβ scores in LNCaP, but obviously more with positive Δβ values in abl (Fig. 6*C*). Thus, CRISPR screens suggest that genes involved in BER pathway, which are also directly targeted by EZH2i, are indispensable for the biological effects of EZH2i in CRPC cells.

To further validate the clinical significance, we examined the expression of these DDR genes in two independent prostate cancer cohorts (25, 26) and found them to be significantly elevated in metastatic CRPC compared to primary prostate tumors (Fig. 6*D* and *SI Appendix*, Fig. S7*D*) and positively correlated with the expression of EZH2 (Fig. 6*E* and *SI Appendix*, Fig. S7*E*). We also associated expression of *EP300*, *FOXA1*, and *AR* with EZH2 dependency or sensitivity to EZH2 inhibitor in all types of cancer cells expressing wild-type EZH2, using the genome-wide CRISPR-Cas9 knockout screen data (27) and the Cancer Therapeutics Response Portal (CTRP) compound screening data (28), respectively (Fig. 6*F*). Strikingly, as a general transcriptional coactivator, *EP300* was highly associated with EZH2 essentiality and cellular responses to EZH2i in cancer cells, even stronger than *EZH2* and *SUZ12*. Taken together, our findings revealed a close connection between the tumor-suppressive activity of EZH2i and DNA repair machinery, which suggests an indication for these compounds as anticancer drugs.

EZH2 Inhibitors Induce the Formation and Accumulation of Persistent and Unrepaired DNA Damage. As the genes involved in the BER pathway were most significantly repressed by EZH2 inhibitors, we determined the levels of apurinic/apyrimidinic (AP) sites in abl cells upon the treatment with GSK126 (Fig. 7*A*). AP sites leading to the formation of DNA single-strand breaks (SSBs) (29) are generated spontaneously or during the early stage of BER (30). If left unrepaired, these SSBs lead to increased levels of double-strand breaks (DSBs) and genotoxic stress (31, 32). Consistently, we detected an over threefold increase in the number of AP sites per 10^5 nucleotides in abl cells following 1 or 3 d of GSK126 treatment, which returned to baseline by day 6 of treatment. Phosphorylation of γH2AX,

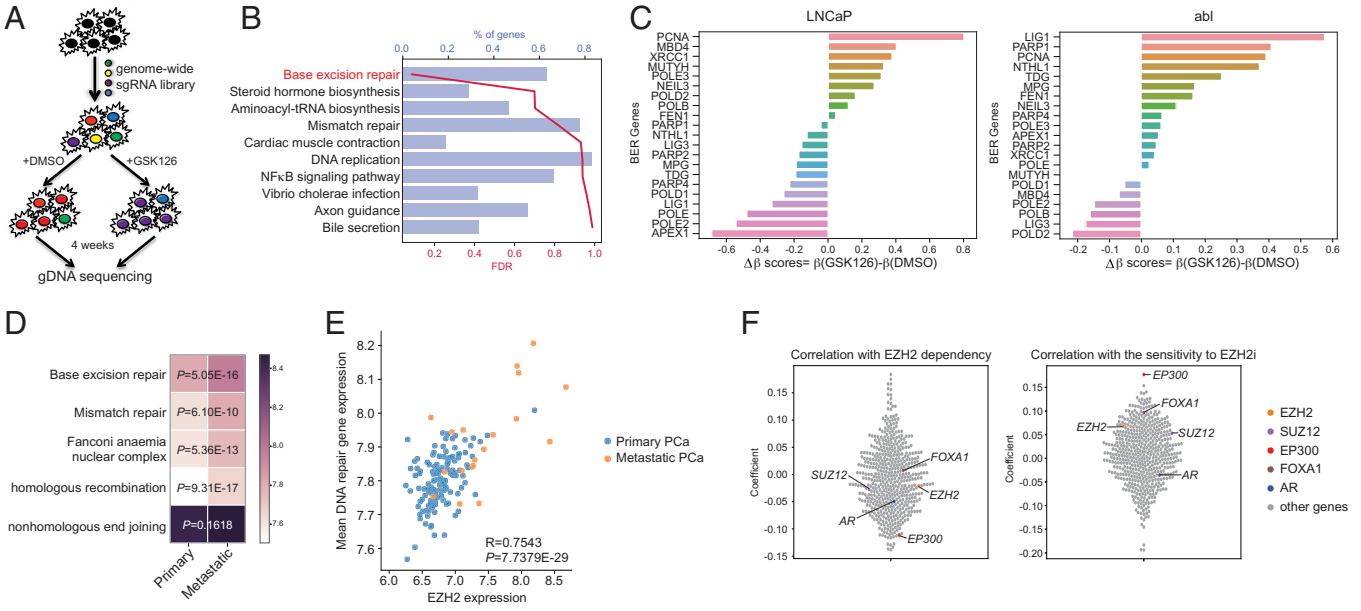

Fig. 6. DNA repair was crucial for the biological effects of EZH2 inhibitors in prostate cancer. (*A*) Workflow of CRISPR-Cas9 knockout screens in LNCaP and abl cells incubated with 1 μM GSK126 for 4 wk. (*B*) Gene set enrichment analysis (GSEA) of genes with positive Δβ, defined as [β (GSK126) − β (DMSO)], in abl cells. (*C*) The Δβ scores for each gene in the BER pathway in LNCaP and abl cells. (*D*) Heat map showing the mean expression (Log2-transformed) of genes involved in each DNA repair pathway in primary (n = 131) and metastatic (n = 19) prostate cancer (25). (*E*) Correlation between expression of EZH2 and the mean expression of DNA repair genes in the same prostate cancer (PCa) cohort as used in *D* (25). Each dot represents a clinical sample. (*F*) Correlation between the expression of indicated genes and EZH2 dependency or sensitivity to EZH2 inhibitor in solid tumor cells expressing wild-type EZH2. *EP300* is significantly correlated with EZH2 dependency (P = 0.003) and EZH2i sensitivity (P = 4E-5). P values were determined by Spearman correlation. EZH2 dependency was calculated using the CERES score in DepMap data (27); the more negative, the more essential. Cellular sensitivity to EZH2 inhibitor (BRD, BRD-K62801835-001-01-0) was calculated using the sensitivity score in CTRP data (28); the more positive, the more sensitive. Gray dots, 500 randomly chosen genes.

which plays a key role in the assembly of DDR proteins at the sites of DSBs (33), increased with prolonged EZH2i treatment concurrent with a decrease in H3K27me3 levels (Fig. 7*B*). Consistent with this observation, immunofluorescence staining of phosphorylated γH2AX revealed the formation of discrete γH2AX foci, an indicator of sites of DSBs (34), inside the nuclei of abl cells 3 d after GSK126 treatment (Fig. 7*C*). The staining increased with prolonged EZH2i treatment and finally manifested in a uniform, widespread pattern over the entire nucleus. Homogeneous, pan-nuclear staining pattern of γH2AX suggests the presence of widespread DSBs and the onset of a preapoptotic signaling (35). Quantification of the numbers of γH2AX foci per cell continuously increased in the presence of GSK126 (*SI Appendix*, Fig. S8*A*), and the pan-nuclear γH2AX staining was more prevalent following 9 to 12 d of incubation with the inhibitor (Fig. 7*D*). Interestingly, the emergence of pan-nuclear γH2AX staining coincided with the disappearance of the accumulated AP sites (Fig. 7*E*), implying a conversion from the spontaneous SSBs to DSBs. Taken together, our results suggest that treatment with EZH2 inhibitors in CRPC cells induces a persistent accumulation of DNA damage, by first leading to increased AP sites and SSBs followed by their conversion to DSBs and genotoxic cell death.

EZH2 Inhibitors Enhance Responses of Prostate Cancer Cells to DNA-Damaging Agents. Our data above provide a rationale for applying EZH2i to sensitize CRPC cells to DNA damage. To validate this, we exposed abl, LNCaP, and DU145 cells to increasing doses of ionizing radiation (IR). While abl cells became much more sensitive to IR after GSK126 treatment (Fig. 8*A*), this difference was very minor in LNCaP (Fig. 8*B*) and did not exist in DU145 (Fig. 8*C*). In addition, we observed drastically delayed DNA repair in abl pretreated with GSK126 (*SI Appendix*, Fig. S8*B*), but not in LNCaP (*SI Appendix*, Fig. S8*C*) or DU145 (*SI Appendix*, Fig. S8*D*). It is worth noting that without EZH2i pretreatment, IR-induced DNA damage was fixed in a much faster rate in abl than in LNCaP and DU145, as unrepaired DNA breaks were significantly less in abl after cell recovery from the treatment with 5 Gy of IR (*SI Appendix*, Fig. S8*E*). This suggests that abl may represent a radioresistant scenario and EZH2i may overcome radiotherapy resistance in advanced prostate cancer.

PARP-1 is an ADP ribosylating enzyme that helps recruit a variety of DNA repair proteins at the sites of DNA damage (36). It has been reported that deficiencies of any components in BER pathway resulted in hypersensitivity of cancer cells to PARP inhibitors (37). We therefore assessed the biological effect of combining EZH2i with the PARP-1 inhibitor olaparib on the proliferation of LNCaP or abl cells. Combined treatment of EZH2i and olaparib greatly suppressed abl cell growth compared to each drug alone (Fig. 8*D*) and showed strong synergistic effect (Fig. 8*E*, *Right*). However, this synergy of EZH2i and olaparib was much milder in LNCaP (Fig. 8*E*, *Left*). Taken together, our work has uncovered a therapeutic strategy for hormone-independent prostate cancer which exploits the suppressive effects of EZH2i on DDR genes to sensitize cancer cells to DNA damaging agents.

Expression of DDR Genes Predicts Sensitivity of Cancer Cells Expressing Wild-Type EZH2 to EZH2 Inhibitors. We next sought to examine whether what we observed in prostate cancer cells can be generalized to other solid tumor cancer types with high level of wild-type EZH2 expression. We excluded DLBCL cells, acute myeloid leukemia cells, and multiple myeloma cells, as these types of hematopoietic cell lines often contain gain- or loss-of-function mutations of EZH2 (5, 38–40). Mutant EZH2

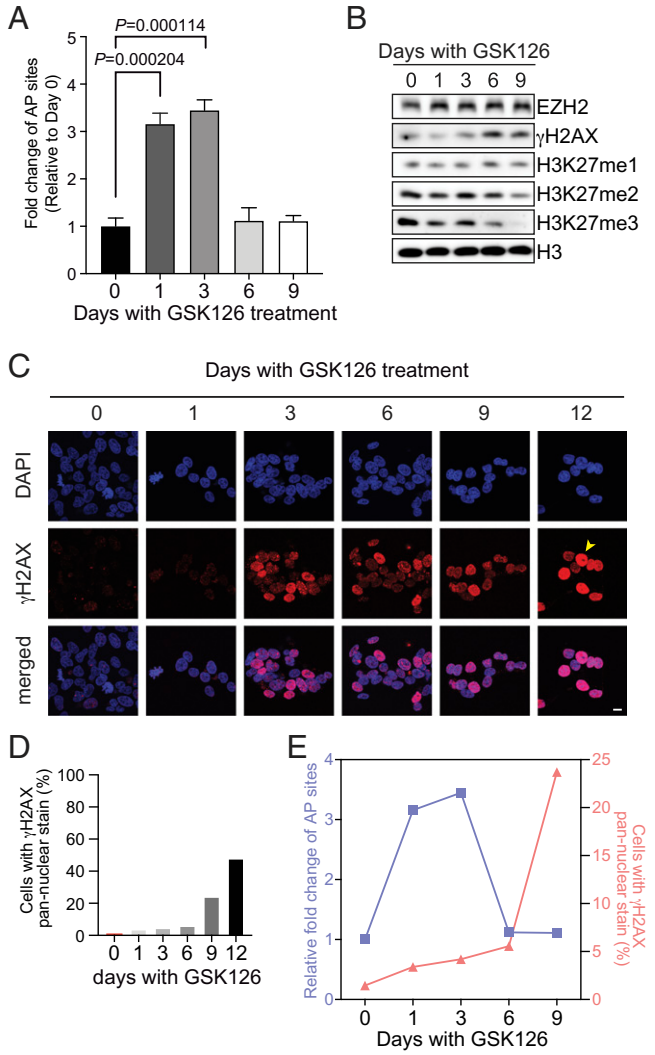

Fig. 7. EZH2 inhibitor induced unrepaired single-strand DNA damage that ultimately triggered DSBs. (*A*) Change of the abasic (AP) sites (relative to day 0) in abl cells treated with 5 μM GSK126. (*B*) Western blot in the nuclear extracts from abl cells treated with 5 μM GSK126. (*C* and *D*) Representative images (*C*) and quantification (*D*) of γH2AX foci in abl cells treated with 5 μM GSK126. Immunofluorescence staining was performed using anti-γH2AX antibody (red) and DNA was stained with DAPI (blue). In *C*, the yellow arrowhead points to a cell with pan-nuclear γH2AX staining. In *D*, data are presented as the average percentages of cells with a solid γH2AX nuclei staining in at least 150 random microscopic views. (Scale bar in *C*, 10 μm.) (*E*) Lines merging the average fold change of AP sites relative to day 0 (blue line) and the average percentages of cells with pan-nuclear γH2AX staining (pink line) in abl cells with 5 μM GSK126 treatment.

in these scenarios has been reported to exert its oncogenic function in a classical H3K27me3-dependent mechanism (5, 41). In addition, mutations in subunits of the SWI/SNF chromatin remodeling complex have been reported to delineate the efficacy of EZH2 inhibitors in certain cancer cells (42–44). Even though prostate cancer cells with mutant SWI/SNF seemed to be more responsive to EZH2 inhibitor, they were equally as dependent on EZH2 for proliferation as those with the wild-type complex (*SI Appendix*, Fig. S9*A*). In all solid tumors expressing wild-type EZH2 (*SI Appendix*, Fig. S9*B*), there were no differences between cancer cells with and without SWI/SNF mutations regarding EZH2 essentiality or sensitivity to EZH2i. Taken together, we excluded solid tumor cell lines with genetic alterations on EZH2 only.

We examined solid tumor cell lines in the Cancer Cell Line Encyclopedia (CCLE) dataset (45) (Fig. 9*A*) and clinical tumors from The Cancer Genome Atlas (TCGA) dataset (46) (Fig. 9 *B* and *C*) and observed a strong expression correlation between wild-type EZH2 and the DDR genes. These results suggest that EZH2-mediated control of DNA repair machinery may represent a common mechanism of EZH2 oncogenic function in solid tumors without EZH2 mutations. To examine whether expression of these DDR genes can dictate EZH2i sensitivities, we analyzed the sensitivities to EZH2i in 531 wild-type EZH2-expressing cancer cells lines in the CTRP compound screening data (28). Across different cancer types, we found that cellular sensitivity to EZH2 inhibitor was significantly and positively correlated with expression of DDR genes (Fig. 9*C*). In comparison with the bottom one-third of cell lines with the lowest levels of DDR genes, the top one-third that express the highest levels of these genes were much more sensitive to EZH2i treatment (*SI Appendix*, Fig. S9*D*). Furthermore, we confirmed that expression of DDR genes dictated EZH2 dependency across 489 cell lines with wild-type EZH2 in the CRISPR-Cas9 knockout screen data (27) (Fig. 9*D*). In contrast, for genes that were repressed by EZH2, although having negative expression correlation with EZH2 (*SI Appendix*, Fig. S9*E*) their levels were not associated with sensitivity to EZH2i (*SI Appendix*, Fig. S9*F*), even across different types of cancer cells (*SI Appendix*, Fig. S9*G*). Taken together, our analyses suggest that the mechanism of inhibitory action of EZH2 inhibitors may be different in solid tumors expressing the wild-type EZH2 from that in hematopoietic malignancies with EZH2 somatic mutations. The group of DDR genes that are directly activated by EZH2 can reliably predict efficacy of EZH2 inhibitors in wild-type EZH2-expressing solid tumors.

Discussion

The methyltransferase EZH2 has been a focus of cancer drug development for several years. Inhibitors of EZH2 have been tested in patients with NHL harboring the gain-of-function mutations of EZH2 (47). However, whether EZH2 inhibitors will have activity in solid tumors expressing high levels of wild-type EZH2 remains an open question. Our study in prostate cancer cells revealed that genetic and pharmacological inhibition of EZH2 directly down-regulates a set of DDR genes. A gene signature based on these EZH2-activated genes underlies the growth-suppressive effects of EZH2 inhibitors in CRPC cells and predicts responses to EZH2 inhibitors across other cancer types with wild-type EZH2. Our findings highlight the important role that the gene activation activity of EZH2 plays in mediating its oncogenic function. More importantly, this unclassical activity of EZH2 defines a potential mechanism of action of EZH2 inhibitors (EZH2i) and lays the mechanistic foundation for the potential clinical applications of EZH2i to sensitize cancer cells to DNA damaging agents.

In this study, we posited a working model of EZH2-mediated gene activation. Our data demonstrated that EZH2-catalyzed methylation of FOXA1 helps facilitate downstream transcriptional activation events. In CRPC cells, exposure of the TAD on EZH2 protein upon its phosphorylation at S21 releases EZH2 from the PRC2 complex and recruits the transcriptional coactivator P300 to the *cis*-regulatory elements of target DDR genes. Thus, the active histone mark H3K27ac is enriched, whereas the repressive histone mark H3K27me3 is depleted, at these chromatin regions. With the assistance of this FOXA1-EZH2-P300 axis, AR is able to drive the transcription of the DDR genes. EZH2 inhibitor treatment dramatically hinders chromatin association of all these factors. This model implies a direction in developing a new class of EZH2

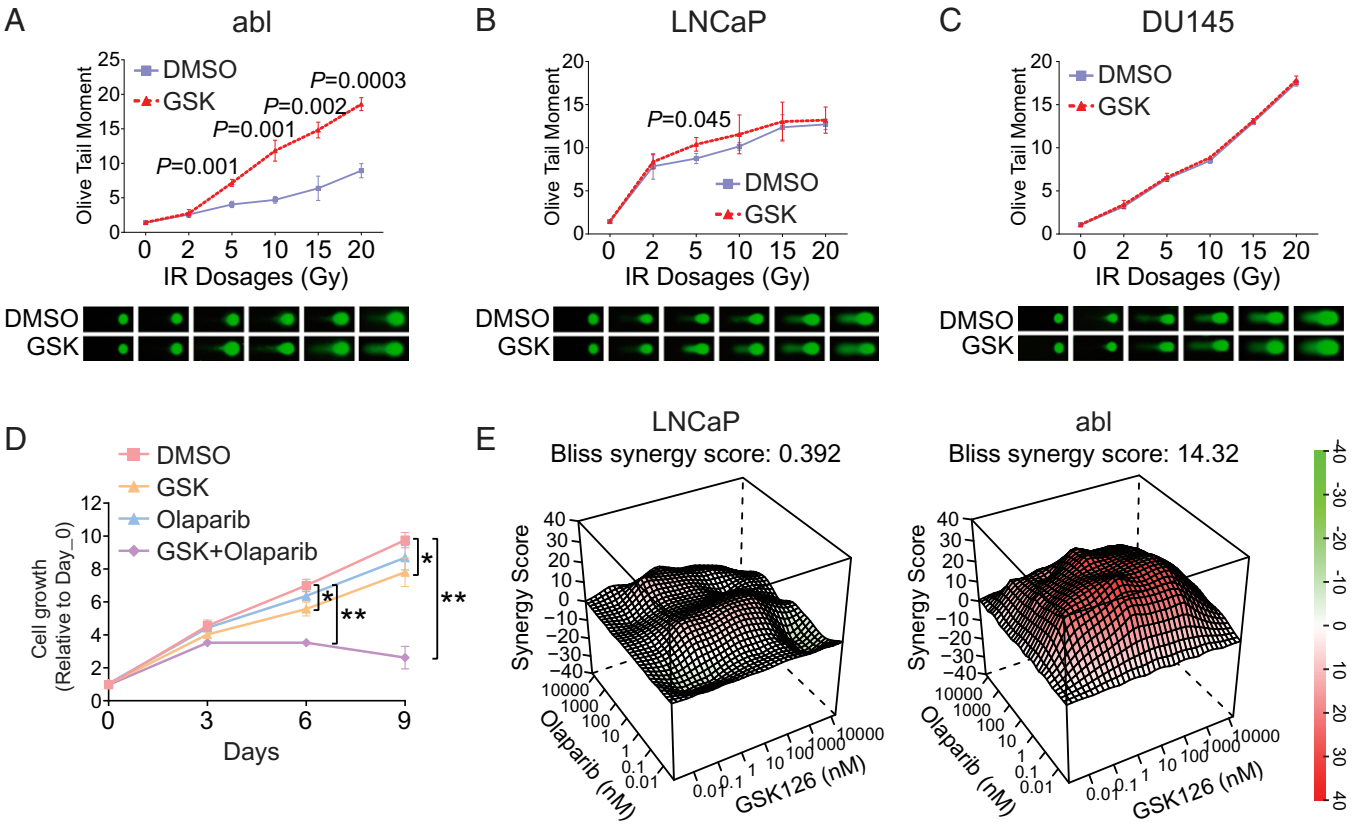

Fig. 8. EZH2 inhibitors enhanced sensitivity of prostate cancer cells to DNA damage agents. (*A–C*) Alkaline comet assays in abl (*A*), LNCaP (*B*), and DU145 (*C*) pretreated with 5 μM GSK126 for 7 d and then exposed to IR followed by recovery for 4 h. (*D*) Growth of abl cells treated with 0.5 μM GSK126, 1 μM Olaparib, or both (GSK+Olaparib). **P* < 0.05; ***P* < 0.01. (*E*) Synergistic effect of EZH2 inhibitor and PARP inhibitor in LNCaP and abl cells incubated with various doses of GSK126 and olaprib for 7 d. A matrix for synergy score was calculated (56).

inhibitors that directly target its gene activation activity, which may be more potent in cancer like CRPC.

CRISPR-based knockout screens revealed that DDR genes, particularly those in the BER, are required for the optimal growth-inhibitory effects of EZH2i in CRPC cells. The expression of these genes was acutely and robustly down-regulated upon EZH2i treatment, and their levels are highly correlated with cellular sensitivities to EZH2i. These findings suggest a different mechanism of action of EZH2 inhibitors in solid tumors with wild-type EZH2 from their action in NHL with gain-of-function mutations of EZH2. In lymphomas, such as DLBCL and FL, tumors with activating somatic mutations of EZH2 are generally more susceptible to EZH2i, which induces a robust transcriptional derepression (48), and presence of these genetic alterations is predictive of EZH2i efficacy. Therefore, we suggest that the EZH2-activated gene signature defined in our study may be useful as a predictive biomarker for response to EZH2i in solid tumors lacking gain-of-function mutations.

Another important implication of our findings is the potential of a combination therapy strategy leveraging the interaction between EZH2 and the DNA repair machinery. Spontaneous DNA SSBs at AP sites rapidly increased following EZH2 inhibitor treatment of CRPC cells. As BER pathway genes, responsible for repairing AP sites (49), were down-regulated by EZH2 inhibitors, the accumulated SSBs can no longer be removed and are converted to the DSBs. Consequently, treatment with EZH2 inhibitors significantly boost the growth-inhibitory effects of DNA-damaging agents such as IR and PARP inhibitors such as olaparib. These suggest combination of EZH2i with genotoxic agents may be a tenable approach in anticancer therapy. Interestingly, the LNCaP-abl CRPC cell line in which we demonstrated the synergistic effects of EZH2 inhibitors and DNA-damaging agents carries a heterozygous deletion of BRCA2 exon 12 (50) and is intrinsically refractory to genotoxic insults. Our data in CRPC cell models and our analysis across hundreds of cancer cell lines suggest that EZH2i may overcome resistance to DNA-damaging agents in advanced cancer and improve the efficacy of olaparib in BRCA-deficient and -proficient tumors. Overall, these findings support the development of combination therapies that include DNA damaging agents and EZH2 inhibitors across a range of cancer types.

In summary, our study elucidated a mechanism of EZH2 inhibitor action in cancer. We identified a core gene signature involving DNA repair as a pharmacological readout of EZH2 inhibitor function. These DDR genes are directly targeted by EZH2i and underlie the antitumor effects of these compounds. Finally, our data suggest that EZH2 inhibition might be an attractive approach to sensitize cancers that overexpress EZH2-activated DDR genes to genotoxic agents.

Materials and Methods

Cell proliferation in the presence of EZH2 inhibitors was measured either using ATPlite Luminescence Assay (PerkinElmer) or by direct counting. RNA-seq libraries were constructed as described previously (15) and ChIP-Rx was performed according to a published protocol (18). CRISPR-Cas9 knockout screens were designed based on the reported literature (51–55) and analyzed following MAGeCK protocol (12). All the animal experiments were approved by the Beth Israel Deaconess Institutional Animal Care and Use Committee. Mice were treated with EZH2 inhibitors for 3 wk. All the genome-wide datasets generated in this study were deposited at the Gene Expression Omnibus database (https://www.ncbi.nlm.nih.gov/geo/) with accession number GSE80240. A detailed description of the materials and methods can be found in *SI Appendix*.

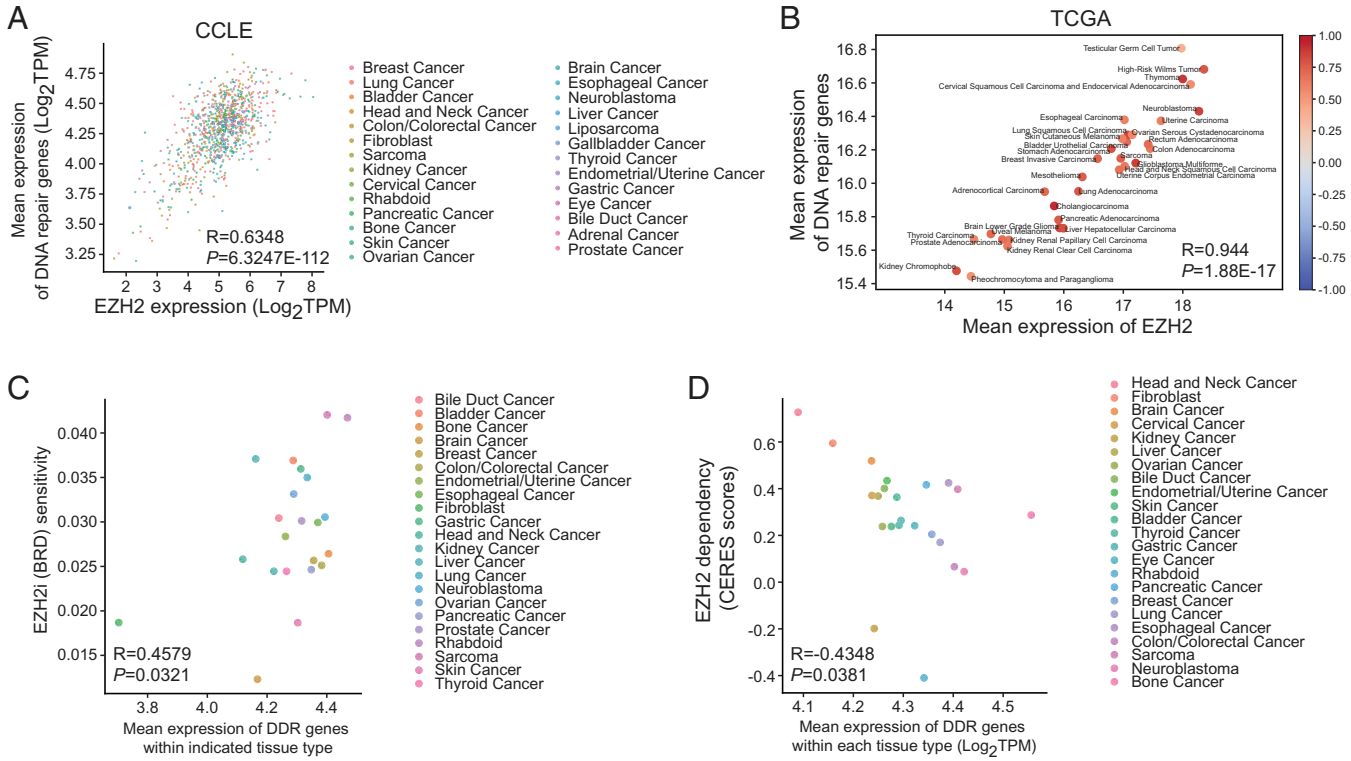

Fig. 9. Levels of DDR genes predict cellular responses to EZH2 inhibitors in multiple types of solid tumors that contain no mutations of EZH2. (*A* and *B*) Correlation between EZH2 expression and the mean expression of DDR genes in cancer cells from CCLE data (45) (*A*) or in patient samples from TCGA (46) (*B*). Each dot represents one cell line (*A*) or one cancer type (*B*). (*C* and *D*) Association between the mean expression of DDR genes and sensitivity to EZH2 inhibitor (*C*) or EZH2 dependency (*D*) in the indicated types of solid tumor cells expressing wild-type EZH2. Sensitivity to EZH2 inhibitor (BRD) and EZH2 dependency were derived from CTRP compound screen data (28) and DepMap CRISPR-Cas9 knockout screening data (27), respectively.

Data Availability. Next-generation sequencing data have been deposited in the Gene Expression Omnibus database (accession no. GSE80240).

ACKNOWLEDGMENTS. We thank Dr. Matthew Freedman, Dr. Zoran Culig, and Dr. Xin Liu for generously sharing their reagents with us. We also thank Anna Groner, Yin Liu, Housheng Hansen He, and Prakash K. Rao for their insightful advice and discussion. This work was supported by grants HG008927 to X.S.L., CA090381 and CA163227 to M.B., and R00 CA178199 to K.X. from the NIH, funding support (PC140817P1 to M.B. and W81XWH-16-1-0409 to N.S.) from the Department of Defense, AACR-AZ START Grant 19-40-12 to N.S., Prostate Cancer Foundation Young Investigator award (to K.X.), a Cancer Prevention and Research Institute of Texas award (RR140072 to K.X.), and a Voelcker Fund Young Investigator award (to K.X.).

1. C. Han Li, Y. Chen, Targeting EZH2 for cancer therapy: Progress and perspective. *Curr. Protein Pept. Sci.* **16**, 559–570 (2015).
2. R. Cao *et al.*, Role of histone H3 lysine 27 methylation in Polycomb-group silencing. *Science* **298**, 1039–1043 (2002).
3. K. H. Kim, C. W. Roberts, Targeting EZH2 in cancer. *Nat. Med.* **22**, 128–134 (2016).
4. M. T. McCabe *et al.*, Mutation of A677 in histone methyltransferase EZH2 in human B-cell lymphoma promotes hypertrimethylation of histone H3 on lysine 27 (H3K27). *Proc. Natl. Acad. Sci. U.S.A.* **109**, 2989–2994 (2012).
5. R. D. Morin *et al.*, Somatic mutations altering EZH2 (Tyr641) in follicular and diffuse large B-cell lymphomas of germinal-center origin. *Nat. Genet.* **42**, 181–185 (2010).
6. M. T. McCabe *et al.*, EZH2 inhibition as a therapeutic strategy for lymphoma with EZH2-activating mutations. *Nature* **492**, 108–112 (2012).
7. S. K. Knutson *et al.*, A selective inhibitor of EZH2 blocks H3K27 methylation and kills mutant lymphoma cells. *Nat. Chem. Biol.* **8**, 890–896 (2012).
8. W. Qi *et al.*, Selective inhibition of Ezh2 by a small molecule inhibitor blocks tumor cells proliferation. *Proc. Natl. Acad. Sci. U.S.A.* **109**, 21360–21365 (2012).
9. L. H. Swift, R. M. Golsteyn, Genotoxic anti-cancer agents and their relationship to DNA damage, mitosis, and checkpoint adaptation in proliferating cancer cells. *Int. J. Mol. Sci.* **15**, 3403–3431 (2014).
10. Z. Wu *et al.*, Polycomb protein EZH2 regulates cancer cell fate decision in response to DNA damage. *Cell Death Differ.* **18**, 1771–1779 (2011).
11. T. Ito, Y. V. Teo, S. A. Evans, N. Neretti, J. M. Sedivy, Regulation of cellular senescence by polycomb chromatin modifiers through distinct DNA damage- and histone methylation-dependent pathways. *Cell Rep.* **22**, 3480–3492 (2018).
12. W. Li *et al.*, Quality control, modeling, and visualization of CRISPR screens with MAGeCK-VISPR. *Genome Biol.* **16**, 281 (2015).
13. C. H. Chen *et al.*, Improved design and analysis of CRISPR knockout screens. *Bioinformatics* **34**, 4095–4101 (2018).
14. D. P. Labbé, M. Brown, Transcriptional regulation in prostate cancer. *Cold Spring Harb. Perspect. Med.* **8**, a030437 (2018).
15. K. Xu *et al.*, EZH2 oncogenic activity in castration-resistant prostate cancer cells is Polycomb-independent. *Science* **338**, 1465–1469 (2012).
16. M. Bisserier, N. Wajapeyee, Mechanisms of resistance to EZH2 inhibitors in diffuse large B-cell lymphomas. *Blood* **131**, 2125–2137 (2018).
17. T. Baker *et al.*, Acquisition of a single EZH2 D1 domain mutation confers acquired resistance to EZH2-targeted inhibitors. *Oncotarget* **6**, 32646–32655 (2015).
18. D. A. Orlando *et al.*, Quantitative ChIP-Seq normalization reveals global modulation of the epigenome. *Cell Rep.* **9**, 1163–1170 (2014).
19. S. H. Park *et al.*, Posttranslational regulation of FOXA1 by Polycomb and BUB3/USP7 deubiquitin complex in prostate cancer. *Sci. Adv.* **7**, eabe2261 (2021).
20. L. Jiao *et al.*, A partially disordered region connects gene repression and activation functions of EZH2. *Proc. Natl. Acad. Sci. U.S.A.* **117**, 16992–17002 (2020).
21. J. Kim *et al.*, Polycomb- and methylation-independent roles of EZH2 as a transcription activator. *Cell Rep.* **25**, 2808–2820.e4 (2018).
22. Y. He *et al.*, FOXA1 overexpression suppresses interferon signaling and immune response in cancer. *J. Clin. Invest.* **131**, e147025 (2021).
23. S. Mei *et al.*, Cistrome Data Browser: A data portal for ChIP-Seq and chromatin accessibility data in human and mouse. *Nucleic Acids Res.* **45** (D1), D658–D662 (2017).
24. B. M. Dancy, P. A. Cole, Protein lysine acetylation by p300/CBP. *Chem. Rev.* **115**, 2419–2452 (2015).
25. B. S. Taylor *et al.*, Integrative genomic profiling of human prostate cancer. *Cancer Cell* **18**, 11–22 (2010).
26. C. S. Grasso *et al.*, The mutational landscape of lethal castration-resistant prostate cancer. *Nature* **487**, 239–243 (2012).
27. A. Tsherniak *et al.*, Defining a cancer dependency map. *Cell* **170**, 564–576.e16 (2017).
28. M. G. Rees *et al.*, Correlating chemical sensitivity and basal gene expression reveals mechanism of action. *Nat. Chem. Biol.* **12**, 109–116 (2016).
29. S. Boiteux, M. Guillet, Abasic sites in DNA: Repair and biological consequences in *Saccharomyces cerevisiae*. *DNA Repair (Amst.)* **3**, 1–12 (2004).

30. A. K. McCullough, M. L. Dodson, R. S. Lloyd, Initiation of base excision repair: Glycosylase mechanisms and structures. *Annu. Rev. Biochem.* **68**, 255–285 (1999).
31. A. Gentil *et al.*, Mutagenic properties of a unique abasic site in mammalian cells. *Biochem. Biophys. Res. Commun.* **173**, 704–710 (1990).
32. D. Kidane, D. L. Murphy, J. B. Sweasy, Accumulation of abasic sites induces genomic instability in normal human gastric epithelial cells during *Helicobacter pylori* infection. *Oncogenesis* **3**, e128 (2014).
33. E. P. Rogakou, D. R. Pilch, A. H. Orr, V. S. Ivanova, W. M. Bonner, DNA double-stranded breaks induce histone H2AX phosphorylation on serine 139. *J. Biol. Chem.* **273**, 5858–5868 (1998).
34. O. A. Sedelnikova, D. R. Pilch, C. Redon, W. M. Bonner, Histone H2AX in DNA damage and repair. *Cancer Biol. Ther.* **2**, 233–235 (2003).
35. S. de Feraudy, I. Revet, V. Bezrookove, L. Feeney, J. E. Cleaver, A minority of foci or pan-nuclear apoptotic staining of gammaH2AX in the S phase after UV damage contain DNA double-strand breaks. *Proc. Natl. Acad. Sci. U.S.A.* **107**, 6870–6875 (2010).
36. H. L. Ko, E. C. Ren, Functional aspects of PARP1 in DNA repair and transcription. *Biomolecules* **2**, 524–548 (2012).
37. J. K. Horton *et al.*, Base excision repair defects invoke hypersensitivity to PARP inhibition. *Mol. Cancer Res.* **12**, 1128–1139 (2014).
38. H. Makishima *et al.*, Novel homo- and hemizygous mutations in EZH2 in myeloid malignancies. *Leukemia* **24**, 1799–1804 (2010).
39. T. J. Ley *et al.*, Cancer Genome Atlas Research Network, Genomic and epigenomic landscapes of adult de novo acute myeloid leukemia. *N. Engl. J. Med.* **368**, 2059–2074 (2013).
40. R. D. Morin *et al.*, Frequent mutation of histone-modifying genes in non-Hodgkin lymphoma. *Nature* **476**, 298–303 (2011).
41. C. Saygin *et al.*, Mutations in DNMT3A, U2AF1, and EZH2 identify intermediate-risk acute myeloid leukemia patients with poor outcome after CR1. *Blood Cancer J.* **8**, 4 (2018).
42. K. H. Kim *et al.*, SWI/SNF-mutant cancers depend on catalytic and non-catalytic activity of EZH2. *Nat. Med.* **21**, 1491–1496 (2015).
43. T. Januario *et al.*, PRC2-mediated repression of SMARCA2 predicts EZH2 inhibitor activity in SWI/SNF mutant tumors. *Proc. Natl. Acad. Sci. U.S.A.* **114**, 12249–12254 (2017).
44. B. G. Bitler *et al.*, Synthetic lethality by targeting EZH2 methyltransferase activity in ARID1A-mutated cancers. *Nat. Med.* **21**, 231–238 (2015).
45. J. Barretina *et al.*, The Cancer Cell Line Encyclopedia enables predictive modelling of anticancer drug sensitivity. *Nature* **483**, 603–607 (2012).
46. The Cancer Genome Atlas Research Network *et al.*, The Cancer Genome Atlas Pan-Cancer analysis project. *Nat. Genet.* **45**, 1113–1120 (2013).
47. N. Gulati, W. Béguelin, L. Giulino-Roth, Enhancer of zeste homolog 2 (EZH2) inhibitors. *Leuk. Lymphoma* **59**, 1574–1585 (2018).
48. R. Tremblay-LeMay, N. Rastgoo, M. Pourabdollah, H. Chang, EZH2 as a therapeutic target for multiple myeloma and other haematological malignancies. *Biomark. Res.* **6**, 34 (2018).
49. M. L. Hegde, T. K. Hazra, S. Mitra, Early steps in the DNA base excision/single-strand interruption repair pathway in mammalian cells. *Cell Res.* **18**, 27–47 (2008).
50. C. Rauh-Adelmann *et al.*, Altered expression of BRCA1, BRCA2, and a newly identified BRCA2 exon 12 deletion variant in malignant human ovarian, prostate, and breast cancer cell lines. *Mol. Carcinog.* **28**, 236–246 (2000).
51. E. P. Garcia *et al.*, Validation of OncoPanel: A targeted next-generation sequencing assay for the detection of somatic variants in cancer. *Arch. Pathol. Lab. Med.* **141**, 751–758 (2017).
52. R. Huether *et al.*, The landscape of somatic mutations in epigenetic regulators across 1,000 paediatric cancer genomes. *Nat. Commun.* **5**, 3630 (2014).
53. M. S. Lawrence *et al.*, Discovery and saturation analysis of cancer genes across 21 tumour types. *Nature* **505**, 495–501 (2014).
54. S. A. Forbes *et al.*, COSMIC: Somatic cancer genetics at high-resolution. *Nucleic Acids Res.* **45** (D1), D777–D783 (2017).
55. B. Vogelstein *et al.*, Cancer genome landscapes. *Science* **339**, 1546–1558 (2013).
56. A. Ianevski, L. He, T. Aittokallio, J. Tang, SynergyFinder: A web application for analyzing drug combination dose-response matrix data. *Bioinformatics* **33**, 2413–2415 (2017).